

Computer Program for the Design of a Countercurrent Moving Carbon Bed Used for the Recovery of Gold from Solutions

J.S.J. VAN DEVENTER and P. JANSEN VAN RENSBURG

Department of Metallurgical Engineering, University of Stellenbosch, Stellenbosch, South Africa

A dual rate kinetic model consisting of differential equations is used to describe the kinetics of the adsorption of gold cyanide on activated carbon. The partial differential equation describing the material balance in the liquid phase is written for the special case of a fixed bed system. It is shown that an isotherm for the case of a closed system is required to yield accurate simulations of the equilibrium in a column of activated carbon. Whereas the equilibrium loading of gold cyanide is influenced by the free access of oxygen to the system, the traditional open batch stirred tank experiments, which are used to estimate parameters for the calculation of breakthrough curves for organic solutes, cannot be used here. The program solves this model at incremental heights in the column at a specific future point in time. Runge-Kutta and backwards-difference methods are used in the numerical solution. A Von Neumann method is used to show that the solution is stable.

Kinetic parameters can be estimated either from batch experiments or from short column runs. In the latter method the column should not be long enough to contain the concentration wavefront for the system of interest. Results obtained from bench scale continuous column experiments were used to verify the computer model. Pure gold solutions as well as real leach liquor were used in both short column and countercurrent moving bed experiments.

Introduction

Adsorption onto activated carbon has found increasing application in the treatment of waste-waters, as well as for the recovery of gold from cyanide leached pulps or clarified liquors. The reactor configurations used are commonly called carbon-in-pulp (CIP), carbon-in-column (CIC) and carbon-in-leach (CIL). The CIC-process is favoured when treating pregnant effluents from a heap leach operation,¹ or plant effluents such as uranium-plant primary filtrate and slimes dam return water.²

Carbon contacting in columns is normally carried out in a fixed-bed, fluidised bed or

countercurrent moving bed. The clarity of the solution, the carbon particle size, the gold content of the solution and the gold loadings to be achieved would largely influence the design and mode of operation. Davidson *et al.*³ have demonstrated how a countercurrent moving bed of carbon could be applied to both clarified pregnant solutions and conventional gold plant pulps.

Although the process design of adsorption in beds of carbon is complex because of the non-steady state of operation, a considerable amount of work has been published on the kinetics and equilibrium of the adsorption

of organics in columns of carbon.⁴⁻⁸ Chen et al.⁹ and Radcliffe⁸ employed a tanks-in-series model to simulate fixed-bed adsorption. Since most industrial scale columns contain some degree of backmixing, the tanks-in-series concept offers a straightforward description of the hydrodynamics in a column. However, when the bed diameter is several orders of magnitude larger than that of the carbon particles, axial dispersion in the liquid phase can be neglected.¹⁰ In this case plug flow may be assumed, which is equivalent to an infinite number of equal-size, small, completely agitated tanks operated in series.⁹ The latter approach will be followed in this paper.

The advantages and disadvantages of the different kinetic adsorption models have been discussed quite extensively for organics⁴⁻⁷ and the gold cyanide complex.¹¹⁻¹² Only some of the principles of the model proposed by Van Deventer¹¹ will be given in the next section.

It is the purpose of this paper to explain the numerical solution of a model for the design of a countercurrent moving carbon bed. Although this system has been studied on pilot plant scale, no basis has been developed for the process design thereof. Bench scale experiments will be used to verify the model.

Mathematical model

Assumptions

As explained by Van Deventer,¹¹ it is customary to assume an internal structure for the carbon. The pores are viewed as either macropores or micropores. Only macropores open onto the external particle surface, whilst the micropores, which branch off the macropores, are responsible for the slow approach to equilibrium. Further assumptions are summarized as follows:

- The carbon particles can be treated as

equivalent spheres.

- Accumulation of gold cyanide in the liquid phase within the pores of the carbon is negligible.
- Equilibrium is assumed to exist between the liquid film surrounding a carbon particle and the gold adsorbed on the external surface of the carbon.
- The rate of transfer across this external liquid film is described by a linear driving force.
- Radial transport in the macropore network can be approximated by a surface diffusion mechanism, especially when adsorption is strongly favoured and relatively dilute solutions are used.¹³ Although pore transport occurs in such instances, its contribution to the total flux is negligible.¹³
- A linear driving force expression is used to describe the rate of diffusion from the macropores to the micropores.¹¹
- The liquid is in plug flow in the countercurrent bed, and the carbon displays a continuous loading distribution along the length of the column.

Material balance equations

Mass transfer in the macropores can be described by the following equation:¹¹

$$\alpha \frac{\partial q_m}{\partial t} = \frac{\alpha D_m}{r^2} \frac{\partial}{\partial r} \left[r^2 \frac{\partial q_m}{\partial r} \right] - k_{mb} (q_m - q_b) \quad \dots [1]$$

According to Hall et al.¹⁴ the loading gradient at the external surface of the carbon can be approximated by a quadratic driving force expression. Eq. [1], may then be approximated by the ordinary differential equation:

$$\alpha \frac{d\bar{q}_m}{dt} = \frac{60\alpha D_m \psi}{d_p^2} \left[\frac{q_s^2 - \bar{q}_m^2}{2\bar{q}_m} \right] - k_{mb} (\bar{q}_m - \bar{q}_b) \quad [2]$$

Hall et al.¹⁴ defined the correction factor ψ in terms of a separation factor which

was dependent on the shape of the adsorption isotherm. Because the parameters D_m and ψ are both functions of the interaction between the adsorbate and the carbon, a combined pseudo surface diffusivity D_m' is defined as:¹¹

$$D_m' = D_m \cdot \psi \quad \dots [3]$$

Equation [2] then becomes:

$$\alpha \frac{d\bar{q}_m}{dt} = \frac{60\alpha D_m'}{d_p^2} \left[\frac{q_s^2 - \bar{q}_m^2}{2\bar{q}_m} \right] - k_{mb}(\bar{q}_m - \bar{q}_b) \quad \dots [4]$$

The mass balance for the micropore region can be written as:¹¹⁻¹²

$$(1 - \alpha) \frac{d\bar{q}_b}{dt} = k_{mb}(\bar{q}_m - \bar{q}_b) \quad \dots [5]$$

A material balance is written at the carbon-liquid interface by equating the surface fluxes:

$$(1 - \epsilon) k_f(C - C_s) = \frac{10\alpha\beta D_m'}{d_p} \left[\frac{q_s^2 - \bar{q}_m^2}{2\bar{q}_m} \right] \quad \dots [6]$$

The equilibrium at the carbon-liquid interface is described by a Freundlich isotherm expression:¹¹⁻¹²

$$q_s = BC_s^b \quad \dots [7]$$

The material balance for a differential element δV of the liquid phase in upward plug flow in a column is:

$$\begin{aligned} In &= Out + Adsorbed + Accumulation \\ \therefore \dot{V}C &= \dot{V}(C + \delta C) + k_f(C - C_s) a_c \delta V \\ &+ \epsilon \delta V \frac{\partial C}{\partial t} \quad \dots [8] \end{aligned}$$

Substitution of $\delta V = A\delta x$ and the total external area of the carbon available in δV , i.e.

$$a_c = \frac{6(1 - \epsilon)}{d_p} \quad \dots [9]$$

into Eq. [8] yields the continuity equation:

$$\dot{V} \frac{\partial C}{\partial x} + \epsilon A \frac{\partial C}{\partial t} + \frac{6k_f(1 - \epsilon)A}{d_p} (C - C_s) = 0 \quad \dots [10]$$

which can be simplified to:

$$\frac{\partial C}{\partial t} + K_1 \frac{\partial C}{\partial x} - K_2(C - C_s) = 0 \quad \dots [11]$$

where

$$K_1 = \frac{\dot{V}}{\epsilon A} \quad \text{and} \quad K_2 = \frac{-6k_f(1 - \epsilon)}{\epsilon d_p}$$

The liquid phase material balance for a batch stirred adsorber is:

$$-V \frac{dC}{dt} = \frac{6k_f W(1 - \epsilon)}{d_p \rho_c} (C - C_s) \quad \dots [12]$$

Numerical solution

Equations [4] to [7], and either [11] or [12], should be solved simultaneously in order to predict carbon loading and liquid phase concentration profiles in a column, or the liquid phase concentration decay curve for a batch stirred adsorber, respectively. Van Deventer¹¹ described the numerical solution for the latter case, and suggested a quadratic transformation of \bar{q}_m in order to remove the singularity which occurs in Eq. [4] when $\bar{q}_m = 0$ at $t = 0$.

Figure 1 shows the logic diagram for the simultaneous solution of Equations [4] to [7] and [11] in the column for a specific future point in time. When the values of C , C_s , q_s , \bar{q}_m and \bar{q}_b have been calculated along the entire column length for such a point in time, the process is repeated for the next point in time.

A value for C_s is needed at every incremental column height for the current future point in time. An initial guess of this value is obtained by assuming that C_s along the entire column length is equal to the values of C_s which have been calculated for the previous moment in time. When the iter-

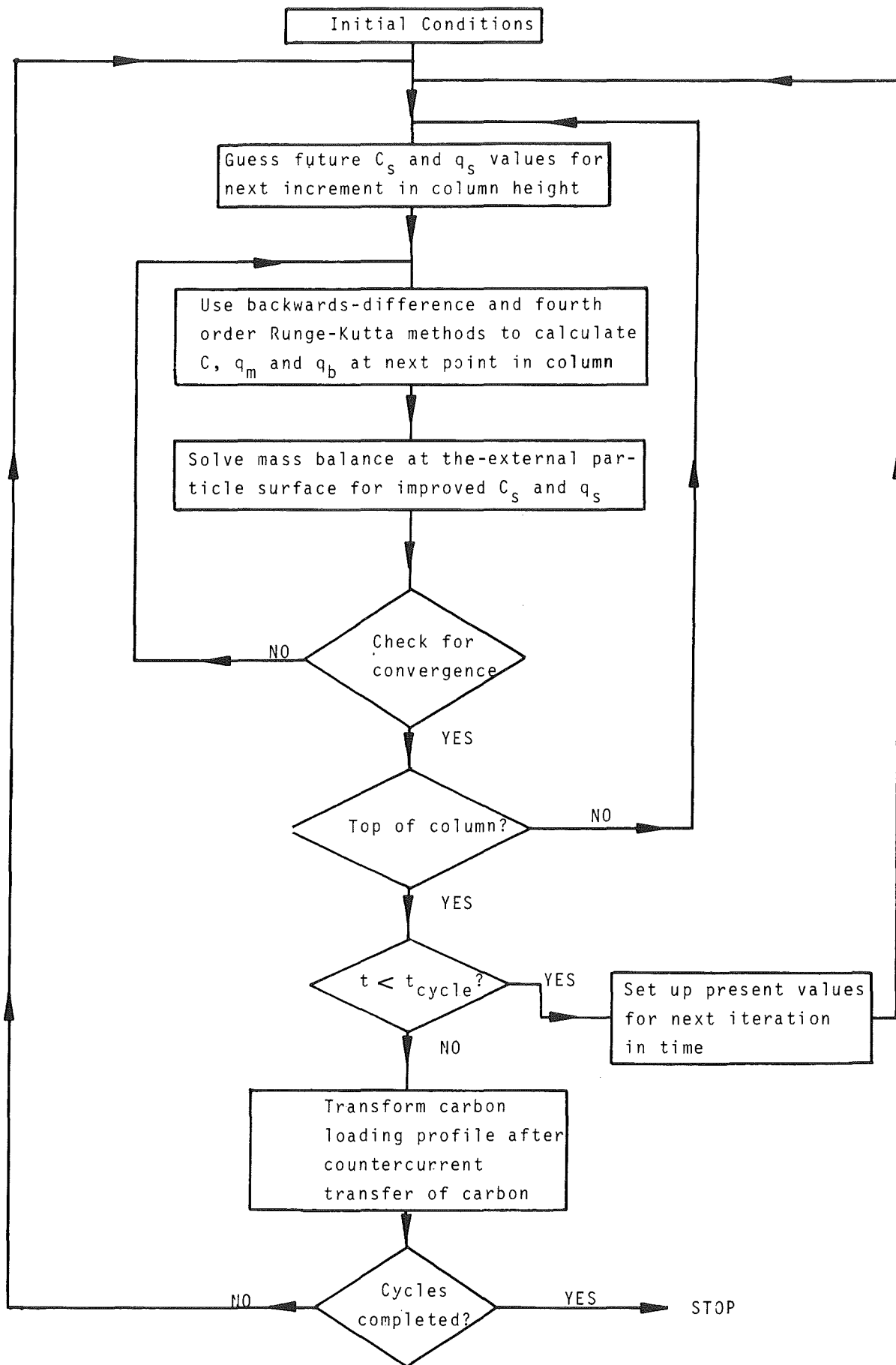


FIGURE 1. Logic diagram for the simulation of a countercurrent moving carbon bed

ation is done for the first time, C_s at each point in the column is assumed to be equal to the value of C_s at the point directly below it at the same point in time. Midtime values for C_s are calculated by averaging present and future values.

The future values of \bar{q}_m and \bar{q}_b are calculated by means of a fourth-order Runge-Kutta routine, where the truncation error of the order k^5 can be neglected by using sufficiently small time step lengths. The Runge-Kutta methods possess the advantage that, since their use at each stage of the advancing calculation does not require information relevant to past stages, they are completely self-starting and are particularly appropriate when memory requirements are to be minimized. These procedures are inherently stable and are such that a change in spacing is effected easily at any stage of the advance.

The liquid phase mass balance, Eq. [11], is a partial differential equation which cannot be solved by Runge-Kutta methods. A backwards-difference scheme can be deduced to approximate the derivatives in Eq. [11]:

$$\begin{aligned} \therefore \left(\frac{1}{k} + \frac{K_1}{h} - K_2 \right) C_{i,n} - \frac{K_1}{h} C_{i-1,n} \\ = \frac{1}{k} C_{i,n-1} - K_2 C_{si,n} \quad \dots [13] \end{aligned}$$

This scheme is used to calculate future values of C , and is stable under all circumstances, as explained in Appendix A.

The liquid film mass balance, as described by Eq. [6], is then solved for C_s by means of the Regula-Falsi method. Convergence is achieved when the fractional difference between the estimated value of C_s , which has been used in the Runge-Kutta and the backwards-difference scheme, and the solution to Eq. [6] lies within the accuracy limit. If convergence is not obtained, the solution to Eq. [6] is used as an improved guess of the

future value of C_s at the current column height, and the process is repeated.

After convergence has been obtained at a particular point in time along the entire column length, the calculated future values of the liquid concentration and the carbon loadings are converted into present values for the next iteration.

When countercurrent removal of carbon takes place, the values of \bar{q}_m and \bar{q}_b are changed to zero for the top fraction of the column where fresh carbon has been added. The values of \bar{q}_m and \bar{q}_b in the bottom fraction of the column are changed to correspond to those values higher up in the column before movement of the carbon had taken place. Calculations are then resumed with these new starting values of gold loading on the carbon.

Estimation of parameters

Weber and Liu¹⁶ proposed the use of a micro-column for the estimation of k_f . In such a column substantial incipient concentration breakthrough occurs, as the length of the column is sufficiently short not to contain the concentration wavefront. A sensitivity analysis¹⁶ showed that, if the packed column is sufficiently short, the initial stage of a breakthrough curve is dominated by film transfer only. Under such circumstances there is no accumulation in an element of liquid in the column, and $C_s = 0$. Therefore Eq. [10] becomes:

$$\epsilon \frac{dC}{dt} + \frac{6k_f}{d_p} (1 - \epsilon) C = 0 \quad \dots [14]$$

when $\dot{V} = \epsilon A \frac{dx}{dt}$. Eq. [14] may be integrated from C_0 at $t = 0$ to C_t at $t = \epsilon AL / \dot{V}$, which yields:

$$k_f = \frac{\ln(C_0/C_t) \dot{V} d_p}{6(1 - \epsilon) AL} \quad \dots [15]$$

The intraparticle kinetic parameters D_m' ,

k_{mb} and α can be estimated from a Powell regression on the concentration decay curve for a batch stirred adsorber, or the breakthrough curve for a packed micro-column. Van Deventer¹¹ explained the estimation of parameters in a batch stirred tank adsorber.

Experimental

The coconut shell carbon used had a wet settled density of 485 kg/m³, a mean particle diameter of 1,66 mm and yielded a voidage of 0,42 in a packed bed. A synthetic potassium aurocyanide solution containing 8,1 ppm gold, and a clarified Witwatersrand cyanide leach liquor containing 7,43 ppm gold were used in all bench scale runs. The pH was maintained at 8,5, the level of dissolved oxygen was 8,2 mg O₂/l in the feed solution and the temperature was 22°C.

Equilibrium and batch stirred tank experiments were conducted both in containers which were open and containers which were closed to the atmosphere, using a stirring speed of 220 rpm, 2,5 l of solution and 0,80 g of carbon. Micro-column runs were conducted in a glass column with an internal diameter of 31 mm, a packed bed height of 5,5 cm and a solution flow rate of 8 l/h. Periodic countercurrent moving bed runs were carried out in a perspex column with an internal diameter of 25 mm, a packed bed height of 34 cm and a solution flow rate of 6 l/h. Carbon was transferred every 24 h when 40% of the carbon bed, i.e. 13,6 cm of the bottom part, was removed while the remainder of the bed was slugged downward and 13,6 cm of fresh carbon added at the top. Care was taken to avoid any mixing of the carbon bed. Samples of solution were taken periodically and analysed for gold by AA.

Application of the model

Figure 2 shows the different equilibrium isotherms and regressed Freundlich expres-

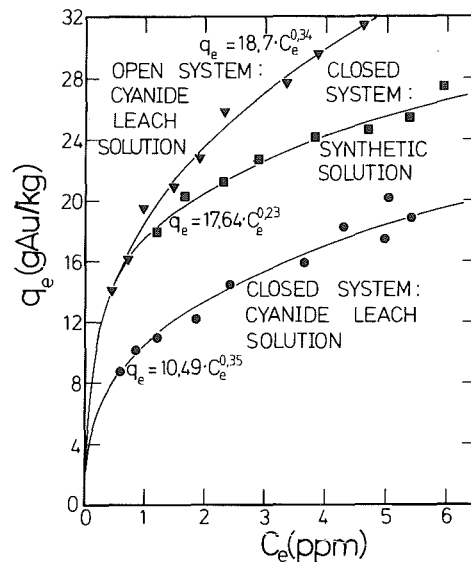


FIGURE 2. Equilibrium adsorption of gold cyanide onto activated carbon

sions. The access of oxygen to an open system causes the equilibrium loading to be significantly higher than that for a closed system. This effect of oxygen has not been considered before in the modelling of adsorption in columns. Neither is it clear how the presence of dissolved oxygen influences the mechanism of adsorption.

Concentration breakthrough curves for the cyanide leach and synthetic solutions in a micro-column are given in Figure 3. Data for the first few minutes have been plotted in Figure 4 and straight lines extrapolated to yield C_t/C_0 intercepts from which k_f could be estimated by use of Equation [15]. A Powell regression of the curves in Figure 3 yielded the intraparticle kinetic parameters given in Table 1 when the isotherm for

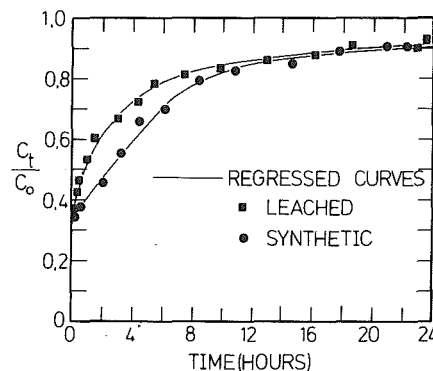


FIGURE 3. Concentration breakthrough curves for micro-column

TABLE 1 Kinetic and equilibrium parameters for different systems

| Parameters | Synthetic gold solution (closed) | Cyanide leach solution | | Sensitivity analysis |
|-----------------------------|----------------------------------|------------------------|------------------------|------------------------|
| | | Open system | Closed system | |
| k_f (m/s) (batch) | - | $5,2 \times 10^{-5}$ | $5,2 \times 10^{-5}$ | - |
| k_f (m/s) (column) | $2,73 \times 10^{-5}$ | $2,52 \times 10^{-5}$ | $2,52 \times 10^{-5}$ | $2,52 \times 10^{-5}$ |
| D_m' (m ² /s) | $8,52 \times 10^{-12}$ | $4,65 \times 10^{-12}$ | $4,65 \times 10^{-12}$ | $4,65 \times 10^{-12}$ |
| k_{mb} (s ⁻¹) | $7,82 \times 10^{-6}$ | $1,20 \times 10^{-5}$ | $1,20 \times 10^{-5}$ | $1,20 \times 10^{-5}$ |
| α | 0,39 | 0,35 | 0,35 | 0,35 |
| b | 0,23 | 0,34 | 0,35 | 0,35 |
| B (g/kg) | 17,64 | 18,72 | 10,49 | 10,49 |
| C_0 (gAu/m ³) | 8,1 | 7,43 | 7,43 | 7,43 |

a closed system was used. It was not possible to obtain a decent simulation of the data points in Figure 3 when the isotherm for an open system was employed. Figure 5 shows batch kinetic data for the cyanide leach solution in both open and closed reactors. The solid lines were predicted by using the parameters estimated from Figure 3 and given in Table 1. It appears as though the same kinetic parameters can be used for both closed and open systems, provided that different isotherms are employed.

Figure 6 shows concentration breakthrough data for the cyanide leach solution fed to the periodic countercurrent moving bed which was operated for four cycles of 24 hours each. The solid lines represent model predictions based on the parameters for open

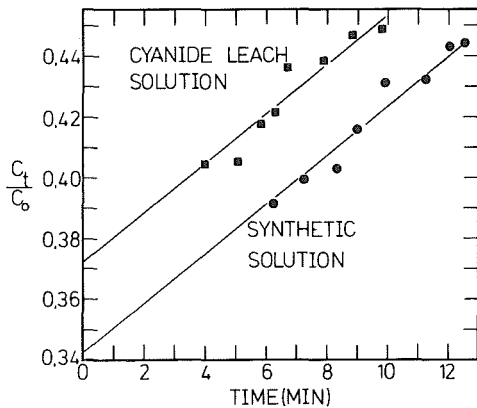


FIGURE 4. Estimation of the liquid film transfer coefficient from micro-column runs

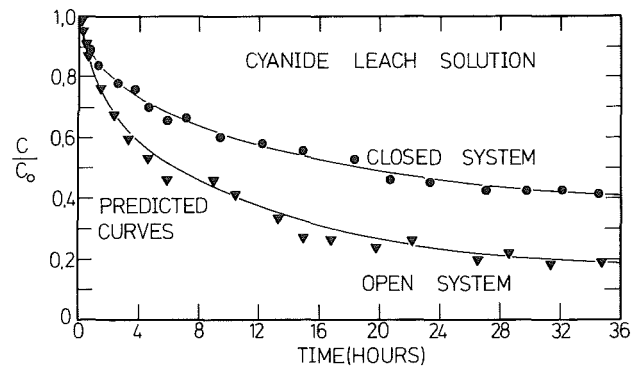


FIGURE 5. Concentration decay curves for batch stirred adsorber experiments

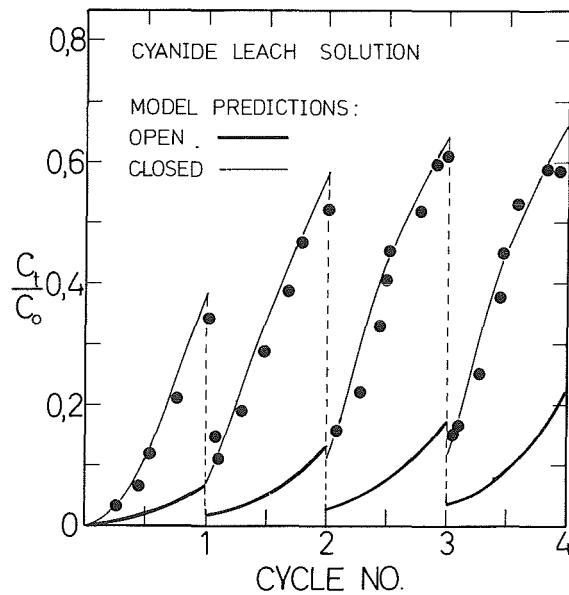


FIGURE 6. Concentration breakthrough curve and model predictions for cyanide leach solution fed to a countercurrent moving carbon bed

and closed systems which are given in Table 1. As could be expected from the regressed curves in Figure 3, only isotherm parameters for a closed system yield satisfactory predictions. The isotherm parameters for an open system predicted unacceptably high loadings on the carbon and therefore too low concentrations in the effluent. This means that the equilibrium conditions in a column of carbon resemble those in a closed stirred tank. Whereas oxygen participates in the adsorption reaction, the traditional approach of estimating parameters in an open stirred tank cannot be used to predict adsorption in columns.

Figure 7 shows that kinetic and equilibrium parameters for a closed system give an accurate prediction of concentration breakthrough of a synthetic gold solution fed to the countercurrent moving bed. As in Figure 6, it was found that a time step length of $k = 5$ min. and an L/h ratio of 30 was sufficient for accurate calculations. Further decreases in k or h did not affect calculations significantly.

Figures 8 to 10 and Table 2 show a sensitivity analysis of the periodic countercur-

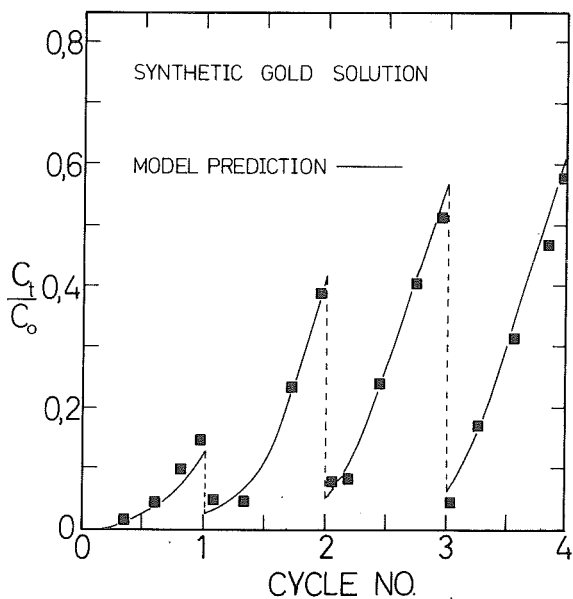


FIGURE 7. Concentration breakthrough curve and model prediction for a synthetic gold solution fed to a countercurrent moving carbon bed

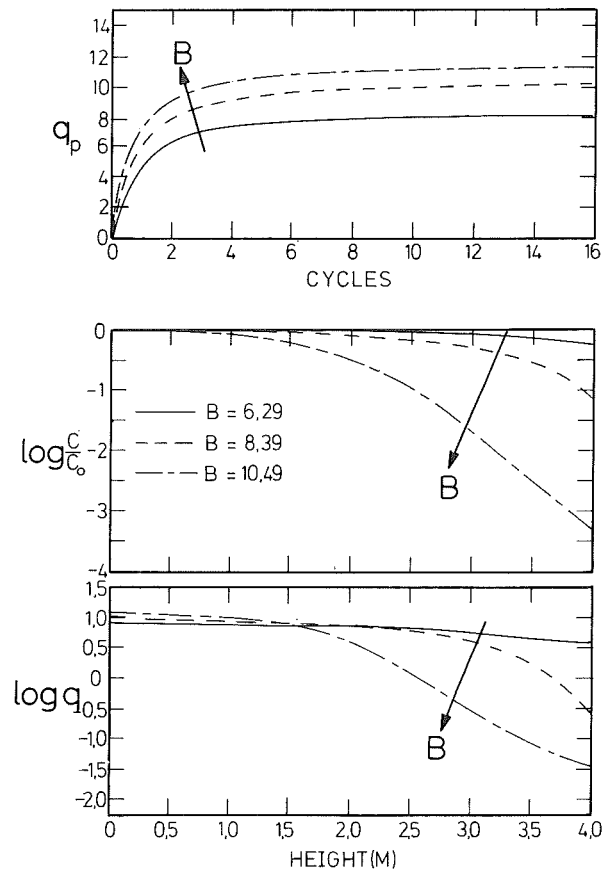


FIGURE 8. Sensitivity of the countercurrent moving bed model to variations in the equilibrium parameter B

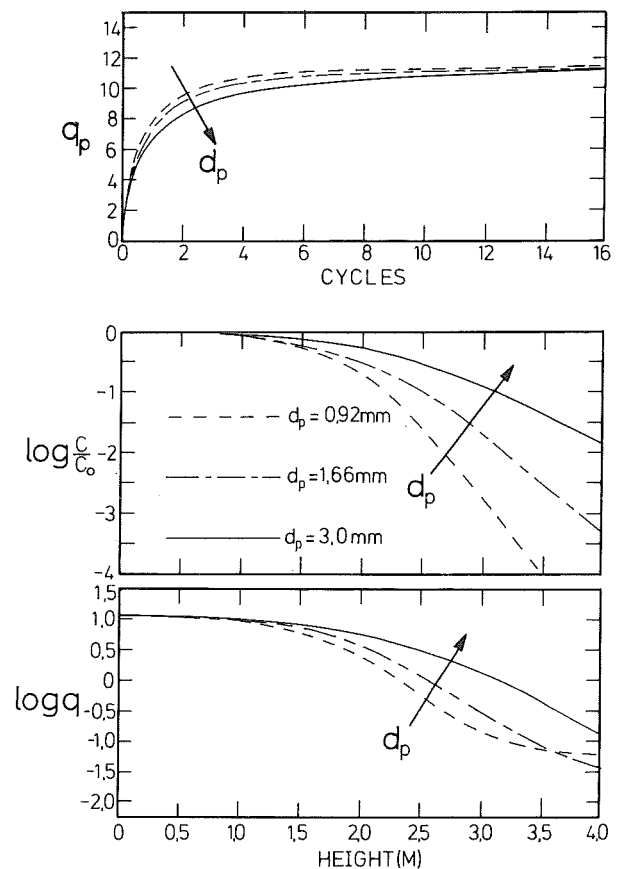


FIGURE 9. Sensitivity of the countercurrent moving bed model to variations in the carbon particle size

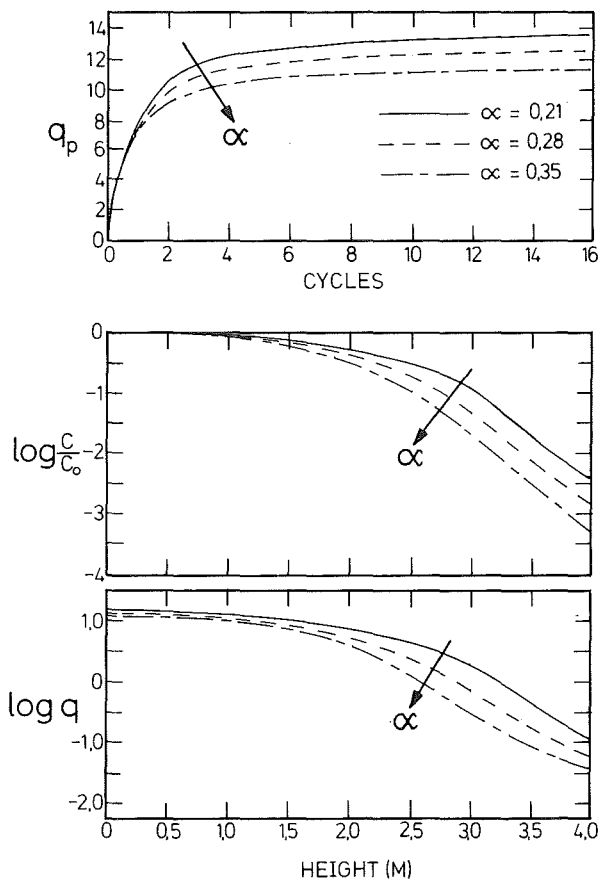


FIGURE 10. Sensitivity of the countercurrent moving bed model to variations in the fraction of adsorptive capacity available as macropores

rent moving bed model based on the appropriate parameters in Table 1, a column length of 4,0 m, a carbon particle size of 1,66 mm, a fractional carbon transfer of 0,2 every 24 hours, and a superficial liquid velocity of 0,61 m/min. As shown for a CIP cascade,¹² an increase in the equilibrium parameter B , a decrease in the particle dia-

TABLE 2

Effect of fractional removal of carbon on adsorption performance (average movement = 0,8 m/day for 30 days)

| Fractional transfer | Duration of one cycle (days) | $\frac{C_t}{C_0}$ | q_p (g/kg) |
|---------------------|------------------------------|-------------------|--------------|
| 0,1 | $\frac{1}{2}$ | 0,0001 | 11,027 |
| 0,2 | 1 | 0,002 | 11,192 |
| 0,4 | 2 | 0,0091 | 12,326 |
| 0,6 | 3 | 0,0312 | 12,15 |

meter, d_p , and an increase in the fraction of loading capacity available as macropores, α , all decrease the concentration of gold in the tailings. The effects of variations in B , d_p or α , are, however, more complex in the case of the countercurrent moving carbon bed than in the case of a CIP cascade. Table 2 shows that, although an increase in the fractional transfer of carbon increases the carbon loading slightly, a concomitant increase in the concentration of gold in the effluent occurs.

Conclusions

The proposed computer program predicted the behaviour of a periodic countercurrent moving carbon bed satisfactorily, and could serve as a basis for the design of such columns. Intraparticle kinetic parameters could be estimated either from batch stirred tank data or from a micro-column run.

Whereas oxygen influences the loading of gold onto carbon, an open stirred tank cannot be used for the prediction of adsorption in a column. Equilibrium conditions in a column of carbon resemble those in a closed stirred tank. A sensitivity analysis showed that an increase in the fractional transfer of carbon increases the concentration of gold in the column effluent.

List of symbols

| | |
|------------|---|
| α_c | Specific external surface area of carbon ($m^2 \cdot m^{-3}$) |
| A | Flow area of column (m^2) |
| b, B | Empirical constants in Freundlich isotherm |
| C | Liquid phase concentration ($g \cdot m^{-3}$) |
| $C_{i,n}$ | C at a specific column height (i) and a specific point in time (n) ($g \cdot m^{-3}$) |
| d_p | Carbon particle diameter (m) |
| D_m | Surface diffusion coefficient ($m^2 \cdot s^{-1}$) |
| D_m' | Pseudo-surface diffusivity in the macropores ($m^2 \cdot s^{-1}$) |

| | |
|-----------|--|
| g | Amplification factor in Eq. [A2] |
| h | Increment in column height (m) |
| k | Increment in time (s) |
| k_f | Liquid film transfer coefficient ($m \cdot s^{-1}$) |
| k_{mb} | Rate coefficient for transfer into the micropores (s^{-1}) |
| L | Height of column (m) |
| \bar{q} | Average loading on carbon (g/kg) |
| r | Radial variable (m) |
| t | Time variable (s) |
| \dot{V} | Volumetric flow rate of liquid ($m^3 \cdot s^{-1}$) |
| V_n | Variable in Fourier series in Eq. [A1] |
| W | Mass of dry carbon (kg) |
| x | Distance variable along column length (m) |

Greek symbols

| | |
|------------|--|
| α | Fraction of loading capacity available as macropores |
| ϵ | Void fraction in packed bed of carbon |
| λ | Parameter in Fourier series |
| ρ_c | Wet settled density of carbon ($kg \cdot m^{-3}$) |
| ψ | Correction factor |

Subscripts

| | |
|---|-------------------------|
| b | Micropores |
| e | Equilibrium |
| m | Macropores |
| o | Initial or feed value |
| p | Product |
| s | Liquid-carbon interface |
| t | Top of carbon bed |

References

- DUNCAN, D.M and SMOLIK, T.J. How Cortez Gold Mine heap-leached low grade gold ores at two Nevada properties. *Engng. Min. J.* vol. 77, July 1977. pp. 65-69.
- DAVIDSON, R.J. and STRONG, B. The recovery of gold from plant effluent by the use of activated carbon. *J.S. Afr. Inst. Min. Metall.* vol. 83, no. 8, 1983. pp. 181-188.
- DAVIDSON, R.J., DOUGLAS, W.D. and TUMILTY, J.A. The recovery of gold from plant solutions by use of a countercurrent moving carbon bed. *J.S. Afr. Inst. Min. Metall.* vol. 85, no. 11, 1985. pp. 387-394.
- McKAY, G. Adsorption of acidic and basic dyes onto activated carbon in fluidised bed. *Chem. Eng. Res. Des.* vol. 61, 1983 pp. 29-36.
- NERETNIEKS, I. Adsorption in finite bath and countercurrent flow with systems having a nonlinear isotherm. *Chem. Eng. Sci.* vol. 31, 1976. pp. 107-114.
- SVEDBERG, U.G. Numerical solution of multicolumn adsorption processes under periodic countercurrent operation. *Chem. Eng. Sci.* vol. 31, 1976. pp. 345-353.
- JOHANSSON, R. and NERETNIEKS, I. Adsorption on activated carbon in countercurrent flow: an experimental study. *Chem. Eng. Sci.* vol. 35, 1980. pp. 979-986.
- RADCLIFFE, D.F. Lumped parameter models of adsorption kinetics in fixed beds. *Chem. Eng. Commun.* vol. 25, 1984. pp. 183-191.
- CHEN, J.W., CUNNINGHAM, F.L. and BUEGE, J.A. Computer simulation of plant-scale multicolumn adsorption processes under periodic countercurrent operation.

- tion. *Ind. Eng. Chem. Proc. Des. Dev.* vol. 11, no. 3, 1972. pp. 430-434.
10. SUNG, E., HAN, C.D. and RHEE, H.-K. Optimal design of multistage adsorption-bed systems. *AIChE J.* vol. 25, no. 1, 1979. pp. 87-100.
 11. VAN DEVENTER, J.S.J. Kinetic model for the reversible adsorption of gold cyanide on activated carbon. *Chem. Eng. Commun.* vol. 44, 1986. pp. 257-274.
 12. VAN DEVENTER, J.S.J. Factors influencing the efficiency of a carbon-in-pulp adsorption circuit for the recovery of gold from cyanided pulps. *PROCEEDINGS OF GOLD 100, VOL. 2: EXTRACTIVE METALLURGY OF GOLD.* Fivaz, C.E. and King, R.P. Johannesburg, SAIMM, 1986. pp. 85-95.
 13. KOMIYAMA, H. and SMITH, J.M. Surface diffusion in liquid-filled pores. *AIChE J.* vol. 20, no. 6, 1974. pp. 1110-1117.
 14. HALL, K., EAGLETON, L.C., ACRIVOS, A. and VERMEULEN, T. Pore- and solid-diffusion kinetics in fixed-bed adsorption under constant-pattern conditions. *Ind. Eng. Chem. Fundam.* vol. 5, no. 2, 1966. pp. 212-223.
 15. SMITH, G.D. *Numerical Solution of Partial Differential Equations: Finite Difference Methods.* 2nd edition, Oxford, Oxford University Press, 1978. pp. 92-95.
 16. WEBER, W.J. and LIU, K.T. Determination of mass transport parameters for fixed-bed adsorbers. *Chem. Eng. Commun.* vol. 6, 1980. pp. 49-59.

Appendix A: Stability of Eq. [11]

A Von Neumann method¹⁵ is used here to prove that the scheme in Eq. [13] is stable. The inherent error in Eq. [13] is written as a discrete Fourier series in the complex exponential form:

$$\left(\frac{1}{k} + \frac{K_1}{h} - K_2\right) V_{n+1} - \frac{K_1}{h} V_{n+1} e^{-\lambda h \sqrt{-1}} = \frac{1}{k} V_n \quad \dots [A1]$$

Substitute $V_{n+1} = gV_n$:

$$g \left[1 + \frac{kK_1}{h} - kK_2 - \frac{kK_1}{h} (\cos \lambda h - \sqrt{-1} \sin \lambda h) \right] = 1 \quad \dots [A2]$$

For stability it is required that $|g| \leq 1$. It must therefore be proven that

$$\left| \left[1 + \frac{kK_1}{h} - kK_2 - \frac{kK_1}{h} \cos \lambda h \right] + \sqrt{-1} \left[\frac{kK_1}{h} \sin \lambda h \right] \right| \geq 1 \quad \dots [A3]$$

$$\therefore \left[1 + \frac{kK_1}{h} - kK_2 - \frac{kK_1}{h} \cos \lambda h \right]^2 + \left[\frac{kK_1}{h} \sin \lambda h \right]^2 \geq 1 \quad \dots [A4]$$

Manipulation of this equation yields:

$$2 \left[\frac{K_1^2}{h^2} - \frac{K_1 K_2}{h} + \frac{K_1}{kh} \right] (1 - \cos \lambda h) + K_2^2 - \frac{2K_2}{k} \geq 0 \quad \dots [A5]$$

Since K_1 is positive and K_2 is negative, Eq. [A5] is valid, and Eq. [A3] is also valid. Therefore, $|g| \leq 1$, so that the scheme in Eq. [13] is stable.